A Novel Substrate Mimetic Inhibitor of PKB/Akt Inhibits Prostate Cancer Tumor Growth in Mice by Blocking the PKB Pathway

Pninit Litman,[‡,§] Osnat Ohne,[‡,§] Shirly Ben-Yaakov,[§] Liron Shemesh-Darvish,[§] Tamar Yechezkel,[§] Yosef Salitra,[§] Shai Rubnov,[§] Ilana Cohen,[§] Hanoch Senderowitz,[§] Dvora Kidron,[ǁ] Oded Livnah,[⊥] Alexander Levitzki,[⊥] and Nurit Livnah*,[§]

DeveloGen Israel Ltd., Kiryat Weizmann, Building 16, Rehovot, Israel 76326, Unit of Pathology, Meir Medical Center, Kfar Saba, Israel, and Wolfson Centre of Applied Structural Biology and Unit of Cellular Signaling, Department of Biological Chemistry, The Alexander Silberman Institute of Life Sciences, Hebrew University of Jerusalem, Jerusalem 91904, Israel

ABSTRACT: We describe a novel, potent peptide substrate mimetic inhibitor of protein kinase B (PKB/Akt). The compound selectively kills prostate cancer cells, in which PKB is highly activated, but not normal cells, or cancer cells in which PKB is not activated. The inhibitor induces apoptosis and inhibits the phosphorylation of PKB substrates in prostate cancer cell lines and significantly increases the efficacy of chemotherapy agents to induce prostate cancer cell death, when given in combination. In vivo, the inhibitor exhibits a strong antitumor effect in two prostate cancer mouse models. Moreover, treated animals develop significantly less lung metastases compared to untreated ones, and the effect is accompanied by a significant decrease in blood PSA [prostate-specific antigen] levels in treated animals. This compound and its potential analogues may be developed into novel, potent, and safe anticancer agents, both as stand-alone treatment and in combination with other chemotherapy agents.

Enhanced PKB/Akt is the hallmark of many aggressive cancers such as breast cancer (*1*, *2*), pancreatic adenocarcinoma (*3*), and gliomas (*4*−*6*). Activated PKB/Akt has been detected in human cancers of the breast, colon, ovary, pancreas, head, neck, and prostate (*7*−*14*). Accumulating evidence implies that PKB[1] is highly significant in the development of prostate cancer and is particularly important in the hormone-refractory stage of the disease (*15*−*18*). Prostate cancer is the second leading cause of cancer mortality in males in the Western world (*19*−*21*), and 25−30% of the prostate cancer tumors behave aggressively, leading to death within 12 months (*22*, *23*). Androgen deprivation therapy is often used for prostate cancer patients; however, the disease may become resistant within months or years. For hormone-resistant prostate cancer, current chemotherapies and radiation treatment offer only palliative effect, with no survival benefit (*24*, *25*). Clinical reports indicate that PKB is significantly overexpressed in prostate tumors compared to benign prostate tissue, and its level is directly correlated with tumor progression and PSA (prostate-specific antigen) serum levels, as well as the Gleason score of the tumors (*13*, *17*, *18*). This evidence suggests that

inhibitors of PKB may be efficient as novel therapeutic agents for prostate cancer. These considerations have prompted us and others to develop agents that either inhibit directly PKB/Akt (*26*, *27*), its activation (*28*), or its effect on mTor (*29*).

In light of the evidence of the central role this kinase plays in prostate cancer, we designed specific PKB inhibitors and characterized them in prostate cancer cell lines, specifically lines lacking PTEN (phosphate and tensin homologue deleted from chromosome Ten) leading to high levels of phosphorylated Akt/PKB. In our previous study (*30*) we described a new series of small molecule ATP mimetic PKB inhibitors. These compounds induce cell death and apoptosis in several cell lines and inhibit the phosphorylation of the PKB/Akt downstream substrate GSK3 in transfected HEK cells. However, the selectivity of these compounds for PKB/Akt over structurally related kinases such as PKA and PKC was relatively low, as is often observed with ATP mimetic compounds (*31*−*34*). The likelihood that ATP competitive inhibitors hit other Ser/Thr kinases is not negligible, especially in view of the existence of about 500 such kinases, let alone other ATP-dependent enzymes. In contrast, substrate mimetic compounds, designed to bind to the protein substrate-binding site, have a much greater potential for selectivity and, therefore, for decreased toxicity (*35*−*37*). These considerations led us to design a series of peptides according to a motif derived from the PKB substrate protein GSK3 (*38*) and use them as the basis for the design of a substrate mimetic PKB inhibitor. Previous attempts to convert substrate peptides into inhibitors using similar approaches (*39*, *40*) have resulted in peptides that were ineffective as potential pharmaceutical agents due to low stability in serum, limited

* To whom correspondence should be addressed. Tel: 972-8-9387774. Fax: 972-8-9300083. E-mail: livnah@develogen.com.
‡ These authors contributed equally to this work.
§ DeveloGen Israel Ltd.
ǁ Meir Medical Center.
⊥ Hebrew University of Jerusalem.
[1] Abbreviations: PKB, protein kinase B; PSA, prostate-specific antigen; PTEN, phosphate and tensin homologue deleted from chromosome; SAR, structure−activity relationship; FKHR, forkhead transcription factor; H&E, hematoxylin and eosin; NHFF, normal human foreskin fibroblasts; ip, intraperitoneal; sc, subcutaneous; IL, interleukin.

bioavailability, and poor cell membrane permeability. In the present study, we have overcome these limitations by chemically modifying the peptide substrate mimetic inhibitors and optimizing their pharmacological properties to yield drug-candidate compounds suitable for systemic administration in animals. The peptides are cell permeable, stable in serum for over 6 h, and slowly metabolized by hepatoma cells. The substrate mimetic peptides are selective for PKB/Akt compared to related kinases, selectively kill cancer cells, but not normal cells, and induce apoptosis and inhibition of PKB/Akt downstream substrate phosphorylation in cells. In vivo, in PC3 and LNCaP mouse xenograft models, systemic administration of the peptide inhibited tumor growth by more than 60% and blocked Akt/PKB activity in the tumor. In addition to the antitumor effect, treatment of the animals resulted in a decrease in the number and size of lung metastases and in a significant decrease in blood PSA levels.

MATERIALS AND METHODS

Preparation of Peptide Solutions for the Various Assays. Stock solutions of peptides at 10 mM concentration were prepared by dissolving the peptides in 100% DMSO and were stored at −20 °C. For each assay, solutions were prepared by diluting the stock solutions to a final concentration of 0.5% DMSO with either doubly distilled H_2O or medium, depending on the assay. This concentration of DMSO was also used in the control samples for all assays.

In Vitro Kinase Activity Assays. (1) PKB Kinase Activity Assays. His-PKBα was prepared as previously described (*41*). A classic radioactive PKB assay was performed using different concentrations of Crosstide peptide (KGRPRTSS-FA) as substrate ($K_m = 2 \mu M$) and 100 μM ATP ($K_m = 155 \mu M$) as previously described (*41*), except that the reaction was carried out for 30 min at 27 °C in order to accommodate a large number of samples.

(2) *The PKA kinase activity assay* was done according to the manufacturer's instructions (Promega) with 5 μM biotinylated Kemptide peptide (biotin-KLRRASLG) and 10 μM ATP.

(3) *PKC and PDK1 kinase activities* were measured using the SignaTECT PKC assay system and PDK1 kinase assay kit according to the manufacturer's instructions (Promega and Upstate Biotechnology, respectively). The ATP concentration for both assays was 10 μM.

(4) *Rock1, CDK2, RAF, and GSK3 kinase activity assays* were carried out at Upstate Biotechnology (KinaseProfiler service) at substrate concentrations which are slightly lower than the K_m of the tested kinase. Fifty percent inhibitory concentration (IC_{50}) values were calculated using nonlinear regression in a one-site competition model with GraphPad Prism version 3.03 Windows (GraphPad Software, San Diego, CA).

Cells and Cell Culture. PC3, LNCaP, A431, and MCF10F cell lines were obtained from the American Type Culture Collection (ATCC). Cells were maintained as indicated by the ATCC. The normal human foreskin fibroblasts (NHFFs) were a gift from InterPharm Laboratories in Israel and were maintained in DMEM supplemented with 10% PBS (all tissue culture reagents were obtained from Biological Industries, Beit Haemek, Israel).

Cell Viability Assays. Normal and tumor cells were plated in 96-well plates, and test compounds were added at various concentrations once the cells were evenly spread at about 50% confluence (24 and 72 h for MCF10F and LNCaP, respectively, 48 h for PC3 and NHFFs). Cell viability was determined after 96 h of incubation with the compounds by staining with 1% methylene blue (Sigma) as previously described (*30*). In combination assays, the dose-dependent curve of mitoxantrone as a single agent was carried out and compared to its activity in the presence of a constant concentration of 2 μM PTR 6164. Both agents were added simultaneously to the culture plate and incubated for 96 h before fixation and staining as described above. Normal peripheral blood lymphocytes (PBLs) were isolated from blood donors using the Ficoll gradient (Novamed), and mononuclear cells were at the interphase. The cells were washed three times in PBS, resuspended in RPMI 1640 medium supplemented with antibiotics, L-glutamine, and 50 μM β-mercaptoethanol, and plated (1.5×10^5 cells per well) in 96-well plates in the presence of 50 units/mL IL-2 (R&D systems) and 5% human serum. Test compounds were added in varying concentrations to the cultured cells, and after 3 days proliferation was detected by measuring the incorporation of [³H]thymidine. Cells were incubated for 5 h with 1 μCi of [³H]thymidine (stock of 5 Ci/mmol; Amersham), harvested on GF/C 96 well plates (Packard), and washed with doubly distilled H_2O, and after addition of scintillation liquid, the radioactivity was counted using a microplate counter (Packard TopCount).

Apoptosis Assay by Caspase Activity. Cells were plated in six-well plates (0.15×10^6 and 0.2×10^6 of PC3 and LNCaP cells, respectively), and after 48 h test compounds were added. After 24 h incubation, the cells were harvested, and apoptosis was measured using in situ FLICA carboxyfluorescein pan-caspase detection kit according to the manufacturer's instructions (Chemicon International Inc.). The activity of the caspases was determined by FACS analysis (FACSCalibur; Becton Dickinson).

Western Blot Analysis. PC3 cells (0.7×10^6) and LNCaP cells (2×10^6) were seeded in 80 cm² flasks and allowed to grow for 3 days in culture before inhibitor compounds were added. After a further 24 h incubation, the cells were lysed in lysis buffer [20 mM Tris-HCl, pH 7.4, 150 mM NaCl, including 0.5% Triton X-100, 25 mM NaF, 2 mM 4-(2-aminoethyl)benzenesulfonyl fluoride (AEBSF), 1 mM sodium orthovanadate, 10 mM β-glycerophosphate, 1 μg/mL aprotonin, and 5 μg/mL leupeptin]. Nonnecrotic tumor tissues were separated from the tumor taken from mice sacrificed at the end of the in vivo efficacy experiment. The cells were filtered through nylon mesh and lysed as described for the cell lines above. Equal amounts of cellular proteins were separated on 4−20% SDS−PAGE, electroblotted to PVDF membranes, and probed with antibodies directed against phospho-Akt (Ser 473), phospho-tuberin (Thr 1462), phospho-FKHR[1] (Thr 24 and Thr 32), phospho-GSK3α/β (Ser 21, Ser 9), phospho-Bad (Ser 136), and phospho-PDK1 (Ser 241) (all antibodies against the phosphorylated proteins were provided by Cell Signaling Technology). Blots were first exposed to antiphosphoprotein antibodies and then stripped (Restore Western blot stripping buffer; Pierce) and reprobed with antibodies against the total specific protein by using antibodies against Akt1 (Upstate), tuberin, FKHR, α/β tubulin (Santa Cruz Biotechnology), and Bad (Cell Signaling Technology) in order to normalize the amount of protein

loaded. Immunoreactive bands were identified using Super-signal West Pico chemiluminescent substrate (Pierce) and visualized using the Kodak Image System 440 (Kodak Digital Science). Photodensitometric analysis of bands was done using Kodak 1D Image analysis software.

Efficacy Study in Tumor Bearing Mice. (1) PC3 Model. The study was carried out by Unibioscreen S.A., Brussels, Belgium. PC3 cells (2.5×10^6 cells in PBS/matrigel, 1:1) were grafted sc in 5−8-week-old male nude BALB/c mice (average weight 20 g), nine mice per treatment group. When the tumor volume reached approximately 60 mm^3 (calculated by the formula length $\times$ width^2 $\times$ 0.4), treatment was initiated by ip injection of test compounds. Treatment was given daily for 21 days, and mice were inspected for an additional 14 days. Mice were weighed twice a week and observed daily for signs of toxicity (abnormal appearance and behavior). At the end of the experiment, the tumors of six sacrificed mice in each group were removed for histological examination. The remaining three tumors were frozen in liquid nitrogen for Western blot analysis as described above.

(2) LNCaP Model. The study was carried out by CellVax S.A., Loos-les-Lille, France. One million LNCaP cells in exponential phase were suspended in PBS containing 20% matrigel and injected sc in the right flank of 5−8-week-old male nude mice. Tumor-bearing mice were randomized before being divided into the experimental groups of 12 mice each. Treatment with the test material injected ip was started (day 0) when the tumor volume reached 60 mm^3 (calculated by the formula length $\times$ width $\times$ depth $\times$ 0.5236), usually about 2 weeks after injection of LNCaP cells, and was given daily for 21 days followed by an observation period of 18 days. At the end of the experiment, blood was collected from the mice in order to determine the PSA level and other biochemical parameters in the sera. After the mice were sacrificed, the tumors and main organs (lung, heart, liver, spleen, and kidney) were removed for histological examination.

Histological Analysis of Tumors. Immediately after the removal of tumors and organs from the mice, tissues were fixed in 4% buffered formalin, routinely processed, and embedded in paraffin. Histological sections, 4 μm thick, were stained by H&E (hematoxylin and eosin) and examined by a trained pathologist, using an Olympus BX50 light microscope. Mitoses and apoptotic bodies were identified morphologically. The number of mitoses and apoptotic bodies per high-power microscopic field (400$\times$) in five randomly selected microscopic fields was counted and recorded. Student's *t*-test was used for evaluation of significance. Metastases located in histological sections of the internal organs were counted, and their maximal diameter was measured.

Determination of Serum PSA. Levels of PSA in the sera (10 μL/sample) of implanted animals were determined using the Immulite 2000 PSA kit (Diagnostic Products Corp.) according to the manufacturer's assay protocol.

RESULTS

Optimization of the Substrate Mimetic PKB/Akt Inhibitor. A rational combinatorial approach was used in order to generate one compound per well peptide libraries, which

Table 1: Best Performing Potent and Selective PKB/Akt Peptide Inhibitors^a

peptide no.	sequence	IC$_{50}$ (PKB) (μM)	IC$_{50}$ (PKA) (μM)
1	Arg-Pro-Arg-Nval-Tyr-DAP-Hol	0.5	>50
2	Arg-Pro-Arg-Nval-Tyr-Ala-Hol	0.32	>10
3	Arg-Pro-Arg-Leu-Tyr-Ser(Me)-NVal	0.32	>10
4	Arg-Pro-Arg-Leu-Tyr-DAP-Hol	0.4	>10
5	Arg-Pro-Arg-NVal-Tyr-Ser(Me)-Abu	0.2	>10
6	Arg-Pro-Arg-NVal-Tyr-Ser(Me)-NVal	0.3	>10

^{a} Three-letter codes for nonnatural amino acids and peptidomimetic residues: Nval, norvaline; DAP, 2,3-diaminopropionic acid; Abu, 2-aminobutyric acid; Ser(Me), methylserine; Hol, homoleucine.
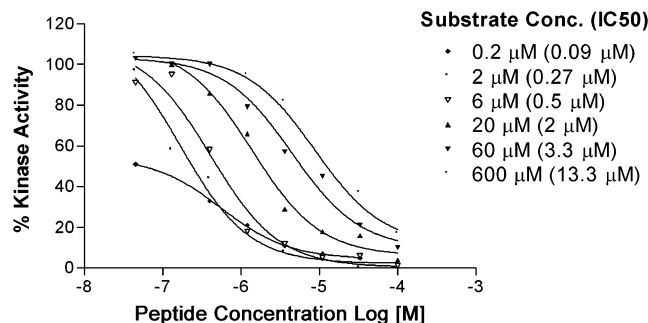

FIGURE 1: Kinetic studies of the substrate mimetic inhibitor peptide 1 in a PKB cell-free kinase assay with different substrate concentrations, demonstrating substrate competitive behavior.

were screened for inhibition of PKB, followed by selectivity screening for PKA and PKC. Starting from the sequence of the GSK3-derived peptide substrate Crosstide, we optimized the peptide length and sequence. Each position was replaced with various natural and nonnatural amino acid residues, according to diversity and similarity considerations, and the serine phosphorylated in the substrate was replaced with nonphosphorylated mimetics (Table 1). As a second step, the successful compounds were further modified for stability and cell permeability. The full SAR of the series is described in Yechezkel et al. (in preparation).

Kinetic Studies of the Substrate Mimetic Inhibitors. In order to define the mode of inhibition of the newly designed PKB/Akt inhibitors, peptide 1 (Table 1) was studied in the presence of increasing concentrations of the PKB substrate Crosstide. Figure 1 shows that the IC$_{50}$ of the inhibitor is directly related to the substrate concentration, due to greater competition with the substrate. The IC$_{50}$ values of the inhibitor ranged from 0.09 μM, in the presence of 0.2 μM substrate, to 13.3 μM, in the presence of 600 μM substrate. In contrast, the calculated K_i values were consistently 112 ($\pm$20) nM, at each of the various substrate concentrations. These results indicate that the inhibitor is acting as a competitive substrate.

The potent and selective PKB substrate mimetic peptide inhibitors depicted in Table 1 were further optimized for stability and cell permeability using various conjugations to hydrophobic moieties. A series of hydrophobic conjugates was screened (data not shown), and from these PTR 6164, which is a cholesterol moiety bound by the hydroxyl group to the N-terminus of peptide 1 (Table 1), was selected for further study. Figure 2 shows a model of PTR 6164 inside the substrate binding site of PKBα. The model was derived
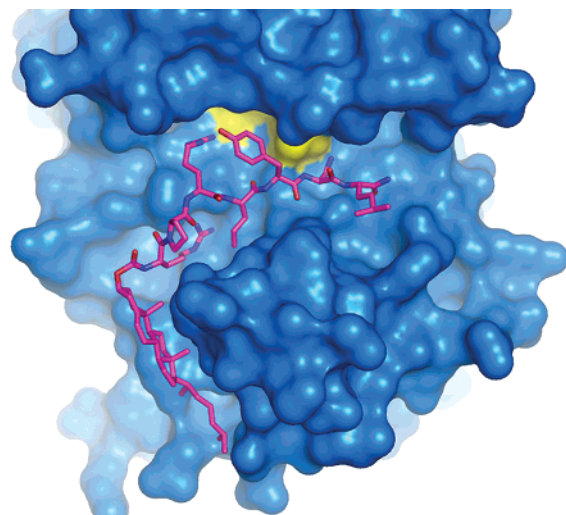
PTR 6164   Cholesteryl-CO-Arg-Pro-Arg-Nval-Tyr-Dap-Hol-NH2

FIGURE 2: Model of PTR 6164 occupying the substrate-binding site of PKBα. Buried residues are indicated in light blue. The ATP site is indicated in yellow. PTR 6164 is positioned in the PKBα crevice between the two kinase lobes. The cholesterol moiety is harbored in a channel, which is approximately at right angles to the main inhibitor peptide. The figure was generated using the PyMol molecular graphics system.

from the crystal structure of PKBβ bound to the GSK substrate peptide (*42*), and PTR 6164 was fitted into the catalytic site based on the fitting of the GSK3 peptide where the identical motif Arg-Pro-Arg in both peptides served as an anchor for fitting the additional segments.

PKB Activity and Selectivity of PTR 6164 in Cell-Free Kinase Assays. PTR 6164 was tested for inhibition of PKB and the structurally related kinases PKA and PKC in a cell-free kinase inhibition assay. While PTR-6164 inhibited PKB at 0.45 μM, PKA and PKC required 6.5 and 5.0 μM, respectively, for inhibition, with 15 μM required to inhibit PDK1. Selectivity was also shown against several other kinases from various families: Rock1 (3 μM), CDK2 (3 μM), RAF (>10 μM), and GSK3 (>10 μM).

PTR 6164 Inhibits Growth of Prostate Cancer Cells by Apoptosis, Concomitant with Inhibition of PKB. The effect of PTR 6164 on cell viability was studied in the prostate cancer cell lines PC3 and LNCaP, containing a high level of activated PKB/Akt, in comparison to a cancer cell line where PKB is not activated, A431, as well as to a normal cell line MCF10F, normal foreskin fibroblasts, and normal peripheral blood lymphocytes (PBLs). PTR 6164 was found to selectively inhibit the growth of prostate cancer cell lines, at low micromolar levels, but showed significantly lower toxicity toward cells where the Akt/PKB is not activated such as A431 cells, MCF10F cells, and normal foreskin fibroblasts (as shown in Figure 3A) or normal blood lymphocytes (Figure 3B), in which PKB activation is either low or absent as previously described (*43*). The level of cell death induced by PTR 6164 in the various cell lines studied seems to correlate with the levels of PKB activation in the cells (Figure 3A). In LNCaP, the endogenous activation of PKB is very high, and these cells were the most susceptible to death induced by PTR 6164 while PC3 cells, in which endogenous PKB activation is moderate, were about 50% less sensitive to the inhibitor. Cells with negligible activation of PKB such as A431 cells and the normal cell line MCF10F

exhibited very low sensitivity. PTR 6164 was not toxic to normal fibroblasts or blood lymphocytes (PBL) at concentrations up to 50 μM (Figure 3B). Prostate cancer cells were incubated for 24 h with PTR6164 and then analyzed for caspase activity. There was a dose-dependent increase in caspase activity (Figure 3C), indicating that the cell death occurs through apoptosis. Further analysis was carried out in order to test if the cell death and apoptosis are concomitant with inhibition of the PKB signaling pathway. Western blot analysis (Figure 3D) shows that treatment of PC3 and LNCaP cells with PTR 6164 in the same concentration range that induced cell death and apoptosis profoundly decreased the phosphorylation of PKB (at residues Ser 473) and its downstream substrates. In LNCaP cells, we show that PTR 6164 significantly inhibits the phosphorylation of four downstream substrates of PKB belonging to various pathways while, in contrast, the phosphorylation of PDK1, which is upstream to PKB, is not inhibited (Figure 3D). The observation for PDK1 is in agreement with the fact that the phosphorylation of residue Thr 308 of PKB, believed to be regulated by PDK1 (*44*, *45*), is not inhibited either. The phosphorylation of Ser 473, however, is decreased and may be attributed to autophosphorylation of PKB, as previously argued (*46*, *47*), although inhibition of upstream proteins suggested to regulate this residue cannot be ruled out. The selectivity of PTR 6164 in inducing prostate cancer cell death as compared to cells devoid of active PKB/Akt, together with the effect on the phosphorylation of PKB/Akt and its downstream substrates, suggests that the compound acts through a targeted process of inhibition of the PKB pathway, rather than through general cell cytotoxicity.

Combination Treatment with PTR 6164 Leads to Increased Cell Death Induction by the Chemotherapy Agent Mitoxantrone. As an apoptosis inducer, a PKB inhibitor is expected to increase the potency of other chemotherapy agents by blocking the survival signal produced by PKB, thus promoting cell death. We studied the cell death induced in LNCaP cells by the commonly used anticancer agent mitoxantrone, as a single agent and in combination with PTR 6164, added at a concentration of 2 μM (4-fold lower than its IC$_{50}$). Figure 4 shows that while mitoxantrone alone induces cell death in LNCaP cells at an IC$_{50}$ of 5 nM, addition of PTR 6164 leads to increased cell death with an IC$_{50}$ of 0.7 nM. The activity of mitoxantrone is thus sensitized by a 7-fold factor, suggesting that PTR 6164 could be useful in combination treatment with other chemotherapy agents.

PTR 6164 Inhibits Growth of Prostate Cancer (LNCaP and PC3) Tumors in Vivo. Prior to the in vivo study, several preliminary in vitro experiments were carried out, aimed to determine the pharmacological fate of this compound after systemic administration. PTR 6164 was found to be stable in mouse plasma for 6 h at 37 °C and slowly metabolized (over 24 h) by human hepatoma cell lines, suggesting liver stability (data not shown). Cell permeability was shown by monitoring a FITC-labeled derivative of PTR 6164 (equipotent to the unlabeled compound in cell-free and cell-based assays) by confocal microscopy (data not shown). These results demonstrated that PTR 6164, despite its peptidic nature, is suitable for systemic administration and may survive in the blood stream and liver passage for a considerable time, allowing efficient distribution to the tumor.
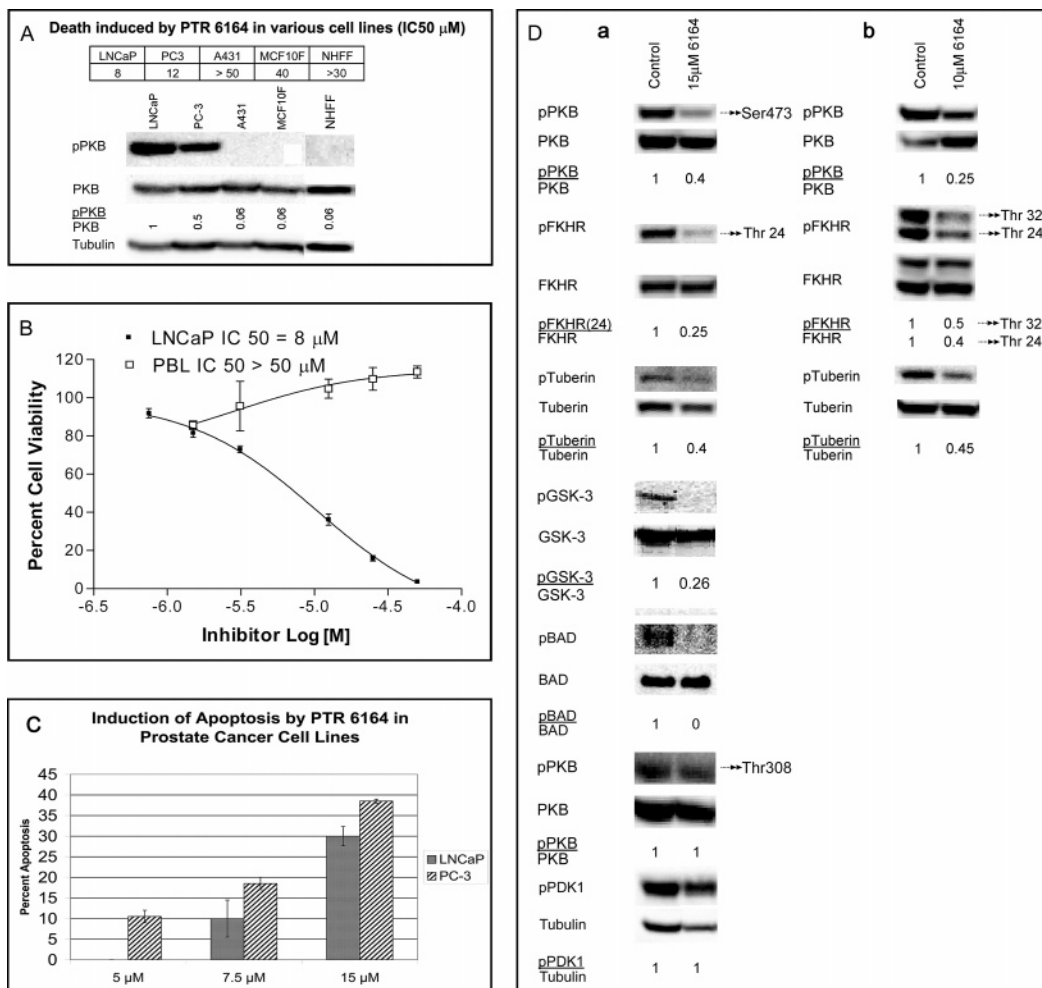
FIGURE 3: Cell death, apoptosis, and inhibition of the PKB pathway in prostate cancer cells are induced by PTR 6164. (A) PTR 6164 induces cell death in prostate cancer cell lines, in which PKB is activated, but not in normal cells or a cancer cell line lacking activated PKB. IC_{50} values of cell death induction, as well as the levels of PKB and p-PKB and the ratio between them, are presented for the various cells. (B) Pronounced selectivity in cell death induced in prostate cancer vs normal blood lymphocytes. (C) Dose-dependent apoptosis is induced by 24 h treatment with PTR 6164, as detected by caspase activity in prostate cancer cells. The number of cells with increased fluorescence intensity (caspase-positive cells) was presented as the percent of the total cells that were counted (10000 cells in each sample). These results imply that the cell death observed occurs through apoptosis. (D) Western blot showing that PTR 6164 inhibits phosphorylation of PKB downstream substrates in two prostate cancer cell lines, PC3 (a) and LNCaP (b). In LNCaP, four downstream substrates of PKB are being inhibited, indicating that the pathway is blocked. In contrast, PDK1, which is upstream to PKB, and its suggested substrate residue Thr 308, are not inhibited. The data are representative of three different experiments in which similar results have been obtained.
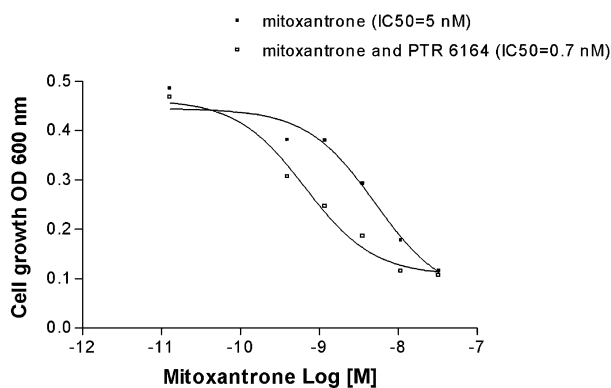
FIGURE 4: Cell viability of LNCaP prostate cancer cells treated with mitoxantrone alone and in combination with PTR 6164. The IC_{50} curve of cell death induction was compared using decreasing concentrations of mitoxantrone as a single agent and, in addition, a constant concentration of 2 μM PTR 6164, leading to a 4-fold increase in the IC_{50} in the combination treatment.

The in vivo effect of PTR 6164 was studied on tumor-bearing nude mice, in two prostate cancer xenograft models,

PC3 and LNCaP. PTR 6164 was administered ip once daily for 21 days to tumor-bearing mice. The animals were further observed for 14 days, subsequent to treatment termination. A significant effect on tumor growth rate was observed in the treated animals, in both PC3 (Figure 5A) and LNCaP (Figure 5B) models, following treatment with 33 and 20 mg/kg inhibitor, respectively. No death, weight loss, or other toxicity signs were observed in any of the animals during the 3 week treatment. Furthermore, after termination of the study, the animals were sacrificed and the organs examined for any abnormalities, first by appearance and then by microscopic analysis of fixed sections. No toxicity markers were observed in any of the organs. In the LNCaP in vivo study, these results were also confirmed by analysis of the plasma retrieved from all mice, indicating normal blood biochemistry profile.

PTR 6164 Decreases the Number and Size of Lung Metastases in Treated Animals in the LNCaP Model. At the end of the in vivo experiment with the LNCaP model, the organs from all animals were subjected to histopathological
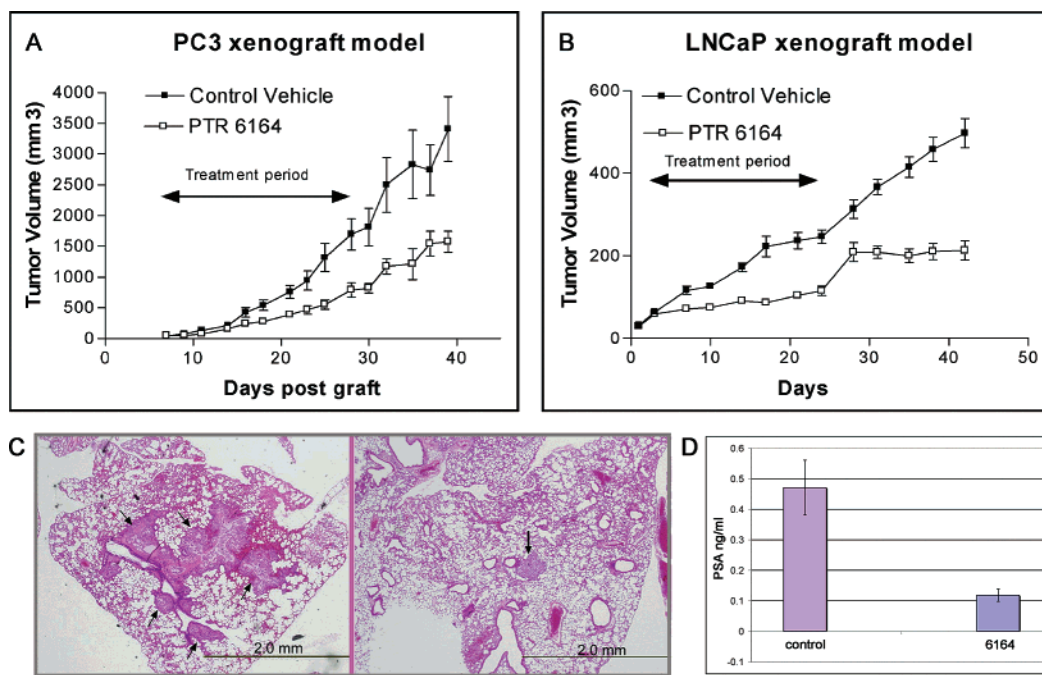
FIGURE 5: PTR 6164 significantly reduces tumor size, lung metastases, and PSA levels in treated prostate cancer tumor-bearing mice. All samples, including tumors, lungs, and plasma, were taken from the mice at the last day of the experiment, and the analyses were done as described in Materials and Methods. (A) In vivo effect on tumor size in the PC3 mouse xenograft model using 33 mg/kg PTR 6164. (B) In vivo effect on tumor size in the LNCaP mouse xenograft model using 20 mg/kg PTR 6164. (C) Lung metastases in the LNCaP model: (left) large pulmonary tumor in the lung of an untreated animal; (right) very small pulmonary tumor in a treated animal. (D) PSA levels in control vs treated animals. A significant decrease in PSA is observed in the treated group.

analysis, revealing metastases in the lungs of the animals. It has been previously reported that LNCaP xenografts may lead to lung metastases (*48*). No metastases were found in the liver, spleen, heart, or kidneys. Among 12 treated animals, 3 animals had lung metastases, compared to 8 out of 12 in the control group. PTR 6164 treatment resulted in a decrease in the number of metastases, with a total of 6 metastases in the treated animals compared to 30 metastases in the control group ($P = 0.05$). A significant decrease in the size of metastases was also induced by the treatment with PTR 6164. The average size was 207 ± 55 μm in the treated group and 386 ± 88 μm in the control group ($P = 0.09$). The combined diameter of all metastases was reduced from 11597 μm in the control group to 1242 μm in the treated group. Representative histological images of pulmonary metastases, showing the differences in metastases size between control and treated animals, are shown in Figure 5C.

PTR 6164 Induces a Decrease in Blood PSA Levels in Treated Mice in the LNCaP Model. Increased PSA levels are associated with prostate cancer development; thus a notable decrease in PSA might imply inhibition of the cancer progression. The LNCaP xenograft model is associated with PSA secretion into the blood and allows monitoring of this human biomarker during the animal study (*49*). In addition to the remarkable effect on tumor growth and on the lung metastases, the LNCaP study reveals a correlation between treatment with PTR 6164 and a decrease in PSA levels in the animals' blood. In the control group, PSA levels were approximately 0.5 ng/mL, while in treated animals, levels were lower than 0.1 ng/mL in most of the animals (Figure 5D). This result is in agreement with clinical reports indicating the correlation between PSA levels and PKB activation in prostate cancer biopsies (*17*).

PTR 6164 Induces Apoptosis and Inhibits PKB Activity in Tumor Cells of Treated Animals. Histological sections of PC3 tumors from treated animals revealed fewer mitoses and more apoptotic bodies per high-power microscopic field in treated animals, in comparison to controls (Figure 6A,B). The difference is statistically significant, with $P = 0.0001$ and $P = 0.006$ for mitoses and apoptosis, respectively. Figure 6B shows that, in the control animals, mitosis was the dominant process with almost 50% more mitotic bodies counted per unit area than apoptotic ones. This ratio was reversed in the treated animals.

In order to relate the antitumor effect of PTR 6164 with the inhibition of PKB/Akt signaling, we examined the effect of the inhibitor on the state of phosphorylated PKB/Akt and its substrates in tumor cells. Tumors were removed from treated and control group mice at the end of the efficacy study, and the tumors cells were analyzed using Western blot. Figure 6C depicts the state of phosphorylation of PKB, FKHR, and tuberin in tumors from three control and three treated mice. It can be seen that phosphorylation of both PKB and its substrates is significantly inhibited in the treated mice compared to the control. This observation suggests that the treatment with PTR 6164 blocks PKB signaling in the tumor cells and may imply that the tumor growth inhibition effect observed in the treated mice is associated with PKB pathway inhibition.

DISCUSSION

In the last several years, cancer research has focused on the development of targeted drugs, which interfere with specific molecular events in tumor development and progression (*36*, *50*). PKB/Akt has been identified as a prime target (*7*, *51*) due to its key role in promoting antiapoptotic
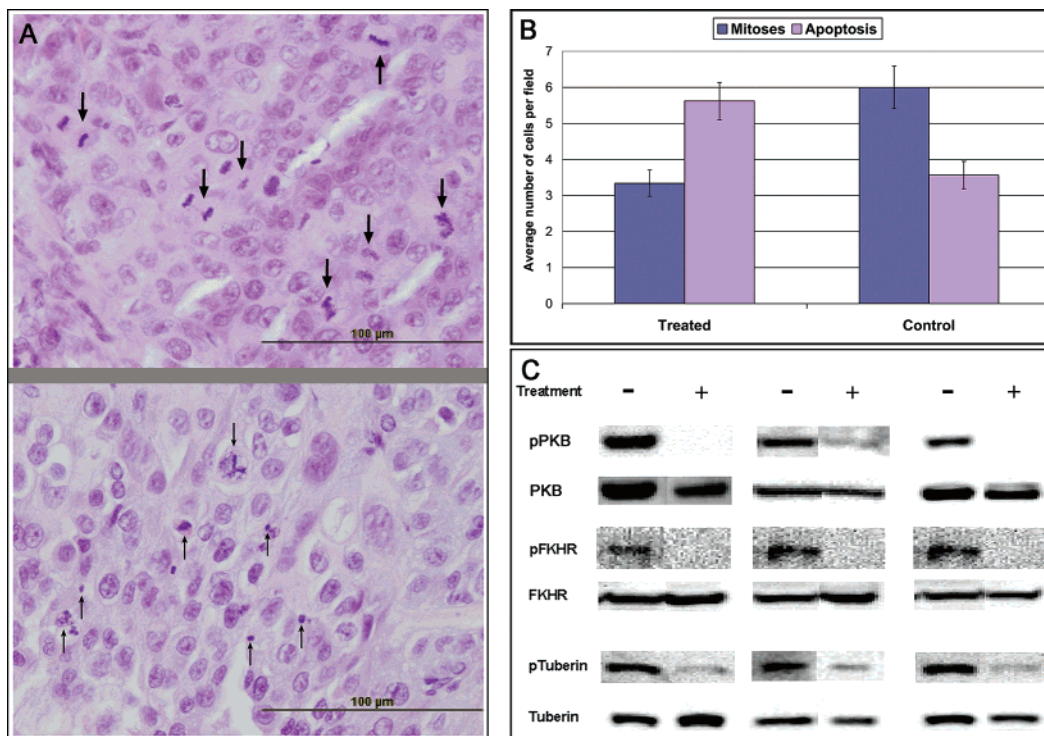
FIGURE 6: Decreased mitosis and increased apoptosis, concomitant with inhibition of PKB signaling, are observed in tumor cells of treated animals from the PC3 study. By the end of the experiment, day 35, which is 2 weeks after the last day of treatment, tumors were taken from each mouse for further analysis. From each experimental group, six tumors were fixed, and histological sections were H&E stained. Apoptotic cells and mitoses were recognized according to their special morphology by an expert histologist. Three sections were made from each tumor, and five microscopic fields were counted in each section as described in Materials and Methods. (A, top) An example of an H&E stained tumor section from a nontreated animal, showing multiple mitotic bodies. (A, bottom) An H&E stained tumor section from a treated animal, showing numerous apoptotic bodies. (B) Mitoses and apoptotic body counts per high-power microscopic field in control and treated animals; average of cells counted in sections made from six tumors in each group (five fields were counted in each section). (C) A decrease in the phosphorylation levels of PKB and its substrates is observed in tumors treated by PTR 6164 compared to untreated tumors, implying inhibition of the PKB pathway associated with the treatment.

pathways, and its inhibition may lead not only to increased death of tumor cells but also to decreased resistance of the tumor to treatment with conventional chemotherapy agents (*52*). Thus, PKB inhibitors may be effective anticancer agents both as stand-alone drugs and in combination therapy.

In this study we have demonstrated, for the first time, the generation of a substrate mimetic inhibitor of PKB/Akt, PTR 6164 (Figure 2), which is highly tolerated and induces profound antitumor effects, both on primary tumor (Figure 5A,B) and on the development of lung metastases in in vivo prostate cancer models (Figure 5C).

PTR 6164 induced strong tumor inhibition in the PC3 (Figure 5A) and LNCaP (Figure 5B) xenograft models where the effect is accompanied by increased apoptosis and decreased mitosis concomitant with in-tumor PKB inhibition (Figure 6). These features make PTR 6164, and its potential analogues, a promising candidate for the treatment of tumors in which PKB/Akt is a prominent antiapoptotic element. The observation that treatment with PTR 6164 significantly reduces the number and the size of lung metastases (Figure 5C) is an exciting and significant result, supporting the potential of this compound as a novel, effective anticancer agent, especially against metastatic prostate cancer, for which no effective treatment is currently available. Our results demonstrate the effect of PTR 6164 on lung metastases, where fewer animals in the treated group had lung metastases compared to the control group. Affected animals in the treated group had significantly less and smaller metastases.

A marked difference was noted in the metastatic load, represented by the combined diameter of all metastases.

PTR 6164 is a peptide-based, substrate mimetic PKB/Akt inhibitor, which is chemically modified for stability and cell permeability. The inhibition through blocking of the substrate site, rather than the highly conserved ATP site, most probably accounts for the compound's potency and selectivity and, therefore, its low toxicity. On the other hand, peptides are often associated with poor pharmacological properties. We have overcome these drawbacks by chemical modifications, including incorporation of nonnatural amino acids and conjugation of nonpeptide hydrophobic moieties. These modifications lead to a peptidomimetic inhibitor that is stable in plasma for over 6 h, is slowly metabolized by hepatoma cells, and is highly cell permeable (Yechezkel et al., in preparation). These favorable properties of PTR 6164 allowed us to study its effects both in cells and in vivo. In this study, we chose to examine prostate cancer cell lines, due to the significant involvement of PKB/Akt in this type of cancer (*13*, *17*, *18*). As clinically observed in prostate cancer patients, there is a direct correlation between the level of PKB activation in the tumor, the Gleason score, and PSA levels (*17*).

PTR 6164 exhibited a remarkable growth inhibitory effect both in vitro and in vivo, concomitant with the inhibition of the PKB/Akt pathway in prostate cancer cells. It induced selective apoptotic cell death in prostate cancer cell lines, correlating well with its potency to inhibit the phosphory-

lation of PKB/Akt downstream substrates, in the low micromolar range (Figure 3). PTR 6164 has very low growth inhibitory effects on normal cells or cells in which PKB activation is negligible (Figure 3). When given in combination with mitoxantrone, PTR 6164 sensitizes the cell death induction activity of mitoxantrone by 7-fold (Figure 4), suggesting that its use in combination treatment could be beneficial.

Interestingly, we have observed in cell lines and in treated tumors a decrease not only in the phosphorylation of PKB substrates but also of the phosphorylation state of PKB at Ser 473, but not at Thr 308. This decrease is unlikely to be due to an effect of PTR 6164 on PDK1, since the IC_{50} of PTR 6164 on PDK1 is 15 μM as compared to 0.47 μM for PKB/Akt (Table 1), and the phosphorylation of PDK1 and of Thr 308, which is believed to be regulated by PDK1 (44, 45), is not inhibited by PTR 6164 (Figure 3D). It is possible that the inhibition of Ser 473 phosphorylation is mediated by PKB/Akt itself by an autophosphorylation mechanism, as suggested by some investigators (46, 47). Other explanations are possible as well. For example, PTR 6164 may also inhibit other enzymes, such as DNA-PK or the complex mTor/Rictor, that have been shown to phosphorylate Ser 473 (53, 54). Another possibility is that the inhibitor binds to the cytoplasmic, unphosphorylated PKB/Akt, thus blocking the phosphorylation of Ser 473. This possibility is supported by the observation that, in our permeability assays, we detect the FITC-labeled PKB/Akt inhibitor (derived from PTR 6164) predominantly in the cytoplasm and not in, or close to, the cell membrane, where PKB/Akt is phosphorylated and activated (data not shown). We can, therefore, hypothesize that the inhibitor acts by binding to the substrate site of the unphosphorylated PKB and inhibits its activation, which would explain the decrease in the phosphorylation of Ser 473 as well as the blocking of the downstream substrate phosphorylation. It should be noted, however, that the screening assay was performed using an activated form of PKB, and therefore one can conclude that PTR 6164 may bind to both the activated and the inactivated forms of the enzyme.

ACKNOWLEDGMENT

REFERENCES

1. Lev, D. C., Kiriakova, G., and Price, J. E. (2003) Selection of more aggressive variants of the gI101A human breast cancer cell line: a model for analyzing the metastatic phenotype of breast cancer, *Clin. Exp. Metastasis 20*, 515−523.

2. Tanner, M., Kapanen, A. I., Junttila, T., Raheem, O., Grenman, S., Elo, J., Elenius, K., and Isola, J. (2004) Characterization of a novel cell line established from a patient with Herceptin-resistant breast cancer, *Mol. Cancer Ther. 3*, 1585−1592.

3. Altomare, D. A., Tanno, S., De Rienzo, A., Klein-Szanto, A. J., Skele, K. L., Hoffman, J. P., and Testa, J. R. (2003) Frequent activation of AKT2 kinase in human pancreatic carcinomas, *J. Cell. Biochem. 88*, 470−476.

4. Ermoian, R. P., Furniss, C. S., Lamborn, K. R., Basila, D., Berger, M. S., Gottschalk, A. R., Nicholas, M. K., Stokoe, D., and Haas-Kogan, D. A. (2002) Dysregulation of PTEN and protein kinase B is associated with glioma histology and patient survival, *Clin. Cancer Res. 8*, 1100−1106.

5. Choe, G., Horvath, S., Cloughesy, T. F., Crosby, K., Seligson, D., Palotie, A., Inge, L., Smith, B. L., Sawyers, C. L., and Mischel, P. S. (2003) Analysis of the phosphatidylinositol 3′-kinase signaling pathway in glioblastoma patients in vivo, *Cancer Res. 63*, 2742−2746.

6. Nakamura, J. L., Karlsson, A., Arvold, N. D., Gottschalk, A. R., Pieper, R. O., Stokoe, D., and Haas-Kogan, D. A. (2005) PKB/Akt mediates radiosensitization by the signaling inhibitor LY294002 in human malignant gliomas, *J. Neurooncol. 71*, 215−222.

7. Kandel, E. S., and Hay, N. (1999) The regulation and activities of the multifunctional serine/threonine kinase Akt/PKB, *Exp. Cell Res. 253*, 210−229.

8. Roy, H. K., Olusola, B. F., Clemens, D. L., Karolski, W. J., Ratashak, A., Lynch, H. T., and Smyrk, T. C. (2002) AKT proto-oncogene overexpression is an early event during sporadic colon carcinogenesis, *Carcinogenesis 23*, 201−205.

9. Vivanco, I., and Sawyers, C. L. (2002) The phosphatidylinositol 3-kinase AKT pathway in human cancer, *Nat. Rev. Cancer 2*, 489−501.

10. Hsu, J., Shi, Y., Krajewski, S., Renner, S., Fisher, M., Reed, J. C., Franke, T. F., and Lichtenstein, A. (2001) The AKT kinase is activated in multiple myeloma tumor cells, *Blood 98*, 2853−2855.

11. Kanamori, Y., Kigawa, J., Itamochi, H., Shimada, M., Takahashi, M., Kamazawa, S., Sato, S., Akeshima, R., and Terakawa, N. (2001) Correlation between loss of PTEN expression and Akt phosphorylation in endometrial carcinoma, *Clin. Cancer Res. 7*, 892−895.

12. Kurose, K., Zhou, X. P., Araki, T., Cannistra, S. A., Maher, E. R., and Eng, C. (2001) Frequent loss of PTEN expression is linked to elevated phosphorylated Akt levels, but not associated with p27 and cyclin D1 expression, in primary epithelial ovarian carcinomas, *Am. J. Pathol. 158*, 2097−2106.

13. Malik, S. N., Brattain, M., Ghosh, P. M., Troyer, D. A., Prihoda, T., Bedolla, R., and Kreisberg, J. I. (2002) Immunohistochemical demonstration of phospho-Akt in high Gleason grade prostate cancer, *Clin. Cancer Res. 8*, 1168−1171.

14. Yuan, Z. Q., Sun, M., Feldman, R. I., Wang, G., Ma, X., Jiang, C., Coppola, D., Nicosia, S. V., and Cheng, J. Q. (2000) Frequent activation of AKT2 and induction of apoptosis by inhibition of phosphoinositide-3-OH kinase/Akt pathway in human ovarian cancer, *Oncogene 19*, 2324−2330.

15. Nakatani, K., Thompson, D. A., Barthel, A., Sakaue, H., Liu, W., Weigel, R. J., and Roth, R. A. (1999) Up-regulation of Akt3 in estrogen receptor-deficient breast cancers and androgen-independent prostate cancer lines, *J. Biol. Chem. 274*, 21528−21532.

16. Ruffion, A., Al-Sakkaf, K. A., Brown, B. L., Eaton, C. L., Hamdy, F. C., and Dobson, P. R. (2003) The survival effect of prolactin on PC3 prostate cancer cells, *Eur. Urol. 43*, 301−308.

17. Liao, Y., Grobholz, R., Abel, U., Trojan, L., Michel, M. S., Angel, P., and Mayer, D. (2003) Increase of AKT/PKB expression correlates with gleason pattern in human prostate cancer, *Int. J. Cancer 107*, 676−680.

18. Zinda, M. J., Johnson, M. A., Paul, J. D., Horn, C., Konicek, B. W., Lu, Z. H., Sandusky, G., Thomas, J. E., Neubauer, B. L., Lai, M. T., and Graff, J. R. (2001) AKT-1, -2, and -3 are expressed in both normal and tumor tissues of the lung, breast, prostate, and colon, *Clin. Cancer Res. 7*, 2475−2479.

19. Trump, D., and Lau, Y. K. (2003) Chemotherapy of prostate cancer: present and future, *Curr. Urol. Rep. 4*, 229−232.

20. Davies, M. A., Koul, D., Dhesi, H., Berman, R., McDonnell, T. J., McConkey, D., Yung, W. K., and Steck, P. A. (1999) Regulation of Akt/PKB activity, cellular growth, and apoptosis in prostate carcinoma cells by MMAC/PTEN, *Cancer Res. 59*, 2551−2556.

21. Martel, C. L., Gumerlock, P. H., Meyers, F. J., and Lara, P. N. (2003) Current strategies in the management of hormone refractory prostate cancer, *Cancer Treat. Rev. 29*, 171−187.

22. Hussain, M., Wolf, M., Marshall, E., Crawford, E. D., and Eisenberger, M. (1994) Effects of continued androgen-deprivation therapy and other prognostic factors on response and survival in phase II chemotherapy trials for hormone-refractory prostate cancer: a Southwest Oncology Group report, *J. Clin. Oncol. 12*, 1868−1875.

23. Kantoff, P. W., Halabi, S., Conaway, M., Picus, J., Kirshner, J., Hars, V., Trump, D., Winer, E. P., and Vogelzang, N. J. (1999) Hydrocortisone with or without mitoxantrone in men with hormone-refractory prostate cancer: results of the cancer and leukemia group B 9182 study, *J. Clin. Oncol. 17*, 2506–2513.

24. Gilligan, T., and Kantoff, P. W. (2002) Chemotherapy for prostate cancer, *Urology 60*, 94–100.

25. Sandler, H. M., Narayan, S., and Smith, D. C. (2003) Combined modality treatment for prostate cancer: role of chemotherapy, *Semin. Oncol. 30*, 95–100.

26. Martelli, A. M., Tazzari, P. L., Tabellini, G., Bortul, R., Billi, A. M., Manzoli, L., Ruggeri, A., Conte, R., and Cocco, L. (2003) A new selective AKT pharmacological inhibitor reduces resistance to chemotherapeutic drugs, TRAIL, all-trans-retinoic acid, and ionizing radiation of human leukemia cells, *Leukemia 17*, 1794–1805.

27. Meuillet, E. J., Ihle, N., Baker, A. F., Gard, J. M., Stamper, C., Williams, R., Coon, A., Mahadevan, D., George, B. L., Kirkpatrick, L., and Powis, G. (2004) In vivo molecular pharmacology and antitumor activity of the targeted Akt inhibitor PX-316, *Oncol. Res. 14*, 513–527.

28. Castillo, S. S., Brognard, J., Petukhov, P. A., Zhang, C., Tsurutani, J., Granville, C. A., Li, M., Jung, M., West, K. A., Gills, J. G., Kozikowski, A. P., and Dennis, P. A. (2004) Preferential inhibition of Akt and killing of Akt-dependent cancer cells by rationally designed phosphatidylinositol ether lipid analogues, *Cancer Res. 64*, 2782–2792.

29. Majumder, P. K., Febbo, P. G., Bikoff, R., Berger, R., Xue, Q., McMahon, L. M., Manola, J., Brugarolas, J., McDonnell, T. J., Golub, T. R., Loda, M., Lane, H. A., and Sellers, W. R. (2004) mTOR inhibition reverses Akt-dependent prostate intraepithelial neoplasia through regulation of apoptotic and HIF-1-dependent pathways, *Nat. Med. 10*, 594–601.

30. Reuveni, H., Livnah, N., Geiger, T., Klein, S., Ohne, O., Cohen, I., Benhar, M., Gellerman, G., and Levitzki, A. (2002) Toward a PKB inhibitor: modification of a selective PKA inhibitor by rational design, *Biochemistry 41*, 10304–10314.

31. Davies, S. P., Reddy, H., Caivano, M., and Cohen, P. (2000) Specificity and mechanism of action of some commonly used protein kinase inhibitors, *Biochem. J. 351*, 95–105.

32. Gumireddy, K., Baker, S. J., Cosenza, S. C., John, P., Kang, A. D., Robell, K. A., Reddy, M. V., and Reddy, E. P. (2005) A non-ATP-competitive inhibitor of BCR-ABL overrides imatinib resistance, *Proc. Natl. Acad. Sci. U.S.A. 102*, 1992–1997.

33. Gumireddy, K., Reddy, M. V., Cosenza, S. C., Boominathan, R., Baker, S. J., Papathi, N., Jiang, J., Holland, J., and Reddy, E. P. (2005) ON01910, a non-ATP-competitive small molecule inhibitor of Plk1, is a potent anticancer agent, *Cancer Cell 7*, 275–286.

34. Godl, K., Wissing, J., Kurtenbach, A., Habenberger, P., Blencke, S., Gutbrod, H., Salassidis, K., Stein-Gerlach, M., Missio, A., Cotten, M., and Daub, H. (2003) An efficient proteomics method to identify the cellular targets of protein kinase inhibitors, *Proc. Natl. Acad. Sci. U.S.A. 100*, 15434–15439.

35. Alfaro-Lopez, J., Yuan, W., Phan, B. C., Kamath, J., Lou, Q., Lam, K. S., and Hruby, V. J. (1998) Discovery of a novel series of potent and selective substrate-based inhibitors of p60c-src protein tyrosine kinase: conformational and topographical constraints in peptide design, *J. Med. Chem. 41*, 2252–2260.

36. Levitzki, A. (2003) Protein kinase inhibitors as a therapeutic modality, *Acc. Chem. Res. 36*, 462–469.

37. Harris, T. E., Persaud, S. J., Saermark, T., and Jones, P. M. (1995) Effects of myristoylated pseudosubstrate protein kinase C peptide inhibitors on insulin secretion, *Biochem. Soc. Trans. 23*, 187S.

38. Alessi, D. R., Caudwell, F. B., Andjelkovic, M., Hemmings, B. A., and Cohen, P. (1996) Molecular basis for the substrate specificity of protein kinase B; comparison with MAPKAP kinase-1 and p70 S6 kinase, *FEBS Lett. 399*, 333–338.

39. Luo, Y., Smith, R. A., Guan, R., Liu, X., Klinghofer, V., Shen, J., Hutchins, C., Richardson, P., Holzman, T., Rosenberg, S. H., and Giranda, V. L. (2004) Pseudosubstrate peptides inhibit Akt and induce cell growth inhibition, *Biochemistry 43*, 1254–1263.

40. Kelemen, B. R., Hsiao, K., and Goueli, S. A. (2002) Selective in vivo inhibition of mitogen-activated protein kinase activation using cell-permeable peptides, *J. Biol. Chem. 277*, 8741–8748.

41. Klein, S., Geiger, T., Linchevski, I., Lebendiker, M., Itkin, A., Assayag, K., and Levitzki, A. (2005) Expression and purification of active PKB kinase from *Escherichia coli*, *Protein Expression Purif. 41*, 162–169.

42. Yang, J., Cron, P., Good, V. M., Thompson, V., Hemmings, B. A., and Barford, D. (2002) Crystal structure of an activated Akt/protein kinase B ternary complex with GSK3-peptide and AMP-PNP, *Nat. Struct. Biol. 9*, 940–944.

43. Nyakern, M., Tazzari, P. L., Finelli, C., Bosi, C., Follo, M. Y., Grafone, T., Piccaluga, P. P., Martinelli, G., Cocco, L., and Martelli, A. M. (2006) Frequent elevation of Akt kinase phosphorylation in blood marrow and peripheral blood mononuclear cells from high-risk myelodysplastic syndrome patients, *Leukemia 20*, 230–238.

44. Sato, S., Fujita, N., and Tsuruo, T. (2002) Interference with PDK1-Akt survival signaling pathway by UCN-01 (7-hydroxystaurosporine), *Oncogene 21*, 1727–1738.

45. Yamada, T., Katagiri, H., Asano, T., Inukai, K., Tsuru, M., Kodama, T., Kikuchi, M., and Oka, Y. (2001) 3-Phosphoinositide-dependent protein kinase 1, an Akt1 kinase, is involved in dephosphorylation of Thr-308 of Akt1 in Chinese hamster ovary cells, *J. Biol. Chem. 276*, 5339–5345.

46. Wick, M. J., Dong, L. Q., Riojas, R. A., Ramos, F. J., and Liu, F. (2000) Mechanism of phosphorylation of protein kinase B/Akt by a constitutively active 3-phosphoinositide-dependent protein kinase-1, *J. Biol. Chem. 275*, 40400–40406.

47. Toker, A., and Newton, A. C. (2000) Akt/protein kinase B is regulated by autophosphorylation at the hypothetical PDK-2 site, *J. Biol. Chem. 275*, 8271–8274.

48. Scatena, C. D., Hepner, M. A., Oei, Y. A., Dusich, J. M., Yu, S. F., Purchio, T., Contag, P. R., and Jenkins, D. E. (2004) Imaging of bioluminescent LNCaP-luc-M6 tumors: a new animal model for the study of metastatic human prostate cancer, *Prostate 59*, 292–303.

49. Lee, C., Sutkowski, D. M., Sensibar, J. A., Zelner, D., Kim, I., Amsel, I., Shaw, N., Prins, G. S., and Kozlowski, J. M. (1995) Regulation of proliferation and production of prostate-specific antigen in androgen-sensitive prostatic cancer cells, LNCaP, by dihydrotestosterone, *Endocrinology 136*, 796–803.

50. Shawver, L. K., Slamon, D., and Ullrich, A. (2002) Smart drugs: tyrosine kinase inhibitors in cancer therapy, *Cancer Cell 1*, 117–123.

51. Hill, M. M., and Hemmings, B. A. (2002) Inhibition of protein kinase B/Akt. Implications for cancer therapy, *Pharmacol. Ther. 93*, 243–251.

52. West, K. A., Castillo, S. S., and Dennis, P. A. (2002) Activation of the PI3K/Akt pathway and chemotherapeutic resistance, *Drug Resist. Updates 5*, 234–248.

53. Sarbassov, D. D., Guertin, D. A., Ali, S. M., and Sabatini, D. M. (2005) Phosphorylation and regulation of Akt/PKB by the rictor-mTOR complex, *Science 307*, 1098–1101.

54. Feng, J., Park, J., Cron, P., Hess, D., and Hemmings, B. A. (2004) Identification of a PKB/Akt hydrophobic motif Ser-473 kinase as DNA-dependent protein kinase, *J. Biol. Chem. 279*, 41189–41196.